changes as dissociation occurs. A more complete description of the mechanisms of metal ion dissociation from polyelectrolyte molecules must await additional studies on the effects of cationic charge, molecular weight, average functional group density of the polyelectrolyte, etc.

Acknowledgment. This research was supported by a contract with the USDOE OBES Division of Chemical Sciences. We are grateful to the Chemistry Division and, particularly, to Dr. James C. Sullivan of the Argonne National Laboratory for making available the facilities for the stopped-flow measurements.

Contribution from the Institut de Chimie Minérale et Analytique, Université de Lausanne, 3 Place du Château, CH-1005 Lausanne, Switzerland

Adducts of Zirconium and Hafnium Tetrachlorides with Neutral Lewis Bases. 2. Kinetics and Mechanism: A Variable-Temperature and -Pressure ^{1}H NMR Study[1,2]

Marianne Turin-Rossier, Deirdre Hugi-Cleary, Urban Frey, and André E. Merbach*

Received June 7, 1989

In CH_2Cl_2 and $CHCl_3$ solution, $ZrCl_4$·2L and $HfCl_4$·2L adducts (L = Lewis base, given in order of increasing adduct stability: Me_2O, $Cl_2(Me_2N)PO$, $Cl(MeO)_2PO$, $(MeO)_3PO$, $Cl(Me_2N)_2PO$) can exist as cis and/or trans isomers. Three reactions can be envisaged in the presence of excess L: (1) *cis*-MX_4·2L ⇄ *trans*-MX_4·2L; (2) *cis*-MX_4·2L + *L ⇄ *cis*-MX_4·L*L + L; (3) *trans*-MX_4·2L + *L ⇄ *trans*-MX_4·L*L + L. Cis–trans isomerization (eq 1) was found to be the fastest reaction and is characterized by a first-order rate law, activation entropies, $\Delta S^{\ddagger}_{i}$, between −49 and +14 J K^{-1} mol^{-1}, activation enthalpies, $\Delta H^{\ddagger}_{i}$, between 48.0 and 67.8 kJ mol^{-1}, and for $ZrCl_4$·2$(MeO)_3PO$ an activation volume, $\Delta V^{\ddagger}_{i}$, of −1.6 cm^3 mol^{-1}. Intramolecular isomerization, with a slightly contracted six-coordinate transition state, was concluded. The second, slower, process observed is intermolecular free ligand exchange on the *trans*- and/or *cis*-MCl_4·2L adducts. When both intermolecular exchanges occur, the exchange on the trans isomer is the faster. The intermolecular exchange reactions were found to obey second-order rate laws, except for MCl_4·2$Cl_2(Me_2N)PO$ (M = Zr, Hf), for which mixed first/second-order rate laws are observed. The second-order intermolecular exchange pathways show very negative $\Delta S^{\ddagger}_{t2}$ and $\Delta S^{\ddagger}_{c2}$ values (−131 to −67 J K^{-1} mol^{-1}), $\Delta H^{\ddagger}_{t2}$ and $\Delta H^{\ddagger}_{c2}$ values between 20.1 and 43.1 kJ mol^{-1}, and for $ZrCl_4$·2$(MeO)_3PO$ a $\Delta V^{\ddagger}_{t2}$ value of −11.1 cm^3 mol^{-1}. An I_a mechanism is suggested, without ruling out a limiting A mechanism. The activation parameters for the first-order cis exchange pathway are interpreted in terms of a limiting D mechanism, which is justified in terms of the stability sequence of the adducts. These results for the $ZrCl_4$·2L and $HfCl_4$·2L adducts contrast with those obtained previously for the $TiCl_4$·2L and $SnCl_4$·2L adducts. For these latter adducts, first, the intermolecular exchange on the cis isomer is much faster than the isomerization and occurs by a D mechanism and, second, the isomerization process itself is characterized by an expanded transition state. This exemplifies the striking differences in reaction mechanism from Ti(IV) and Sn(IV) to Zr(IV) and Hf(IV) metal chloride adducts, MCl_4·2L, due to the increase in ionic radius, which favors the changeover from a bond-breaking to a bond-making mechanism.

Introduction

In the previous paper,[3] we showed that $ZrCl_4$·2L and $HfCl_4$·2L adducts with neutral Lewis bases, L, can exist in CH_2Cl_2 and $CHCl_3$ in the cis form, the trans form, or as an equilibrium of both cis and trans isomers. This was in contrast to the situation for $TiCl_4$·2L adducts,[4] where the cis adduct strongly predominated, except for those adducts with tetrahydrofuran and the strong donors $(MeO)_3PO$, $Cl(Me_2N)_2PO$, and $(Me_2N)_3PO$. However, it is akin to the situation for $SnCl_4$·2L,[5,6] where the cis–trans isomerization equilibrium is observed in most cases.

Three reactions can be envisaged in the presence of both *cis*- and *trans*-MCl_4·2L isomers (M = Sn, Ti, Zr, Hf) and an excess of L. The first reaction is the cis–trans isomerization process:

$$cis\text{-}MX_4\cdot 2L \underset{}{\overset{k_i}{\rightleftharpoons}} trans\text{-}MX_4\cdot 2L \qquad (1)$$

The second and third reactions involve the exchange of free ligand on the cis and trans isomers:

$$cis\text{-}MX_4\cdot 2L + {}^*L \overset{k_c}{\rightleftharpoons} cis\text{-}MX_4\cdot L{}^*L + L \qquad (2)$$

$$trans\text{-}MX_4\cdot 2L + {}^*L \overset{k_t}{\rightleftharpoons} trans\text{-}MX_4\cdot L{}^*L + L \qquad (3)$$

In the previous studies on the $3d^0$ $TiCl_4$·2L[7] and the $4d^{10}$ $SnCl_4$·2L[8-10] adducts only the two first reactions (eqs 1 and 2) were observed. The faster reaction was intermolecular exchange on the cis adduct. Both reactions had first-order rate laws and positive activation entropies and volumes. D mechanisms, with five-coordinate intermediates, were concluded for the intermolecular cis substitution. Intramolecular processes, with expanded six-coordinate transition states, were assigned to the isomerization reactions on the basis of smaller, but still positive, activation volumes. This implies that there is little or no direct intermolecular ligand exchange on the trans isomer (eq 3); rather trans substitution is accomplished through three elementary processes: isomerization to the cis isomer, very fast intermolecular ligand exchange on that isomer, and finally isomerization again to the trans isomer.

Zr^{4+} (ionic radius r = 80 pm[11]) and Hf^{4+} (81 pm) are much larger ions than Ti^{4+} (68 pm) and Sn^{4+} (71 pm), and thus, one may expect large differences in the isomerization and substitution behavior of their MCl_4·2L adducts. The connection between metal ion size and a dissociative–associative changeover in substitution mechanism is well-known for di- and trivalent metal centers.[12,13] Therefore, in order to provide complete mechanistic assignments, variable-concentration, variable-temperature, and variable-pressure kinetic measurements were undertaken for a series of $ZrCl_4$·2L and $HfCl_4$·2L adducts.

(1) Part 43 of the series High-Pressure NMR Kinetics. Taken, in part, from the Ph.D. thesis of M.T.-R.
(2) For part 42, see: Helm, L.; Merbach, A. E.; Kotowski, M.; van Eldik, R. *High-Pressure Res.* **1989**, *2*, 49.
(3) Turin-Rossier, M.; Hugi-Cleary, D.; Merbach, A. E. *Inorg. Chim. Acta* **1990**, *167*, 245.
(4) Turin, E.; Nielson, R. M.; Merbach, A. E. *Inorg. Chim. Acta* **1987**, *134*, 67.
(5) Ruzicka, S. J.; Merbach, A. E. *Inorg. Chim. Acta* **1976**, *20*, 221.
(6) Ruzicka, S. J.; Merbach, A. E. *Inorg. Chim. Acta* **1977**, *22*, 191.
(7) Turin, E.; Nielson, R. M.; Merbach, A. E. *Inorg. Chim. Acta* **1987**, *134*, 79.
(8) Ruzicka, S. J.; Favez, C. M. P.; Merbach, A. E. *Inorg. Chim. Acta* **1977**, *23*, 239.
(9) Knight, C. T. G.; Merbach, A. E. *J. Am. Chem. Soc.* **1984**, *106*, 804.
(10) Knight, C. T. G.; Merbach, A. E. *Inorg. Chem.* **1985**, *24*, 576.
(11) Shannon, R. D. *Acta Crystallogr., Sect. A* **1976**, *A32*, 751.
(12) Ducommun, Y.; Merbach, A. E. In *Inorganic High Pressure Chemistry: Kinetics and Mechanism*; van Eldik, R., Ed.; Elsevier: Amsterdam, 1986; Chapter 2.
(13) Merbach, A. E. *Pure Appl. Chem.* **1987**, *59*, 161.

0020-1669/90/1329-1374$02.50/0

Experimental Section

Sample Preparation. Dimethyl ether, Me_2O (Fluka, puriss), trimethyl phosphate, $(MeO)_3PO$ (Fluka, practical) and hexamethylphosphoramide, $(Me_2N)_3PO$ (Fluka, practical), were dried by using standard methods.[3] The following mono- and dichloro derivatives of $(MeO)_3PO$ and $(Me_2N)_3PO$ were synthesized: $Cl(MeO)_2PO$;[14] $Cl(Me_2N)_2PO$;[15] $Cl_2(Me_2N)PO$.[16] Manipulation of MCl_4 (M = Zr, Hf) and their adducts was described in a previous paper.[3] For the rate law studies, the MCl_4 concentration varied between 0.01 and 0.1 m (m = mol kg^{-1} solvent) and the total added ligand concentration was between 0.03 and 1.0 m. For the determination of the activation parameters, a [metal chloride]:[total ligand] ratio of from 1:3 to 1:5 was chosen by using solutions 0.025–0.10 m in MCl_4 and 0.15–0.50 m in total added ligand. The solvents used were mixtures of normal and deuterated $CHCl_3$, CH_2Cl_2, and $(CHCl_2)_2$.

Variable-Temperature and -Pressure NMR Spectroscopy. The variable-temperature ^1H NMR measurements were made at 60, 200, and 400 MHz with Bruker WP-60, CXP-200, and WH-400 spectrometers, respectively. At 60 MHz 20–100 scans of 4096 points were accumulated over a sweep width of 720 Hz, at 200 MHz 4–20 scans of 8192 points were accumulated over a sweep width of 2000 Hz, and at 400 MHz 10–20 scans of 8192 points were accumulated over a sweep width of 4000 Hz. In all cases the field was locked by using the deuterium solvent signal. Variable-pressure measurements were made by using home-built probes working at 200 MHz (without a field frequency lock)[17] and at 400 MHz (with an internal deuterium lock).[18] The temperature was measured with a Pt resistor for both ambient[19]- and variable-pressure[20] measurements. All ^1H chemical shifts are referenced to TMS.

Two-dimensional ^1H-EXCSY spectra were obtained at 400 MHz by using a phase-sensitive NOESY pulse sequence. The initial relaxation delay was set to 15 s, which is about 5 times the longitudinal relaxation time, and the mixing time was 0.25 s. In the f_2 dimension we used 1024 data points, resulting from eight scans accumulated over a total spectral width of 400 MHz. The f_1 dimension contained 256 words zero-filled to 512. The data were processed by using a Lorentz–Gauss transformation in both dimensions, and the exchange rates were obtained with the D2DNMR program.[21]

Rate Constant Determination. In the slow-exchange region the rate constants were determined from the peak width at half-height of the ^1H NMR signals. For a system with n sites, the residence time, τ_j^r, for a given nucleus in site j is given by $1/\tau_j^r = \pi(W_j - W_j^\circ)$, where W_j and W_j° are the full width at half-height in the presence and absence of exchange, respectively.

In the case of intermediate and fast exchange the spectra were least-squares fitted to the calculated spectrum, using a program derived from EXCNG.[22] The exchange matrices used included $^3J(^1H-^{31}P)$ spin–spin coupling for the phosphoryl ligands. Up to three residence times were simultaneously adjusted to take into account the three reactions given by eqs 1–3: $1/\tau_i^r$ (*cis*-MX_4·2L → *trans*-MX_4·2L); $1/\tau_c^r$ (*cis*-MX_4·2L → free L); $1/\tau_t^r$ (*trans*-MX_4·2L → free L). The chemical shifts and coupling constants used in the calculations have been previously tabulated.[3] Their temperature dependence has also been taken into account. Magnetic field inhomogeneity and instability were accounted for by measuring the width of the TMS reference peak, which was in the range of 0.2 to 1 Hz for the variable-temperature measurements and 1.0 to 2.5 Hz for the variable-pressure measurements (up to 5 Hz at 200 MHz without lock).

Results

For the MCl_4·2L adducts investigated in this kinetic study, $ZrCl_4$·2Me_2O, $ZrCl_4$·2$Cl_2(MeO)PO$, and $ZrCl_4$·2$Cl_2(Me_2N)PO$ exist only as cis isomers, whereas the $ZrCl_4$·2L adducts with L = $(MeO)_3PO$, $Cl(MeO)_2PO$, and $Cl(Me_2N)_2PO$ and the $HfCl_4$·2L adducts with L = $(MeO)_3PO$, $Cl(MeO)_2PO$, $Cl(Me_2N)_2PO$, and $Cl_2(Me_2N)PO$ show equilibria between cis and trans isomers. The electron donor strength order of the phosphoryl ligands is $(Me_2N)_3PO \gg Cl(Me_2N)_2PO > (MeO)_3PO \gg Cl(MeO)_2PO > Cl_2(Me_2N)PO$.

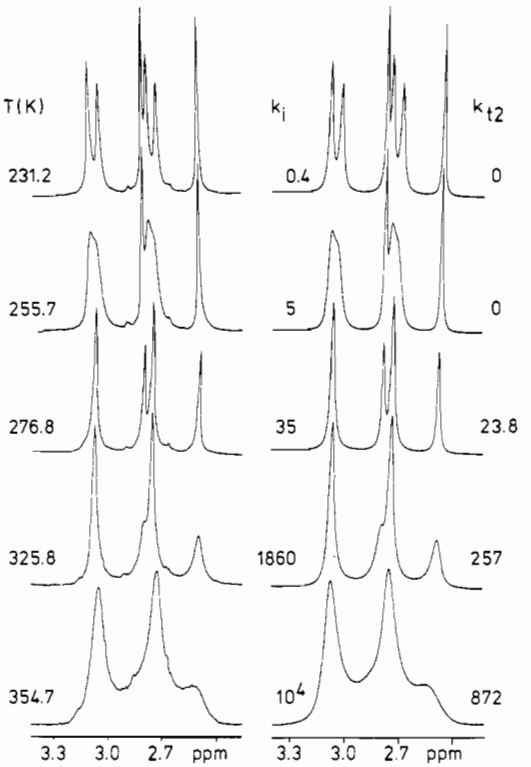

Figure 1. Variable-temperature 60-MHz ^1H NMR spectra of *cis*- and *trans*-$ZrCl_4$·2$Cl(Me_2N)_2PO$ with excess ligand in $CHCl_3$, showing cis–trans isomerization and trans–free ligand exchange. A least-squares fitting program was used to calculate the spectra on the right (k_i in s^{-1} and k_{t2} in s^{-1} m^{-1}). At 231.2 K, where there is almost no exchange, the peak assignments (with the $^3J(^1H-^{31}P)$ coupling constants given in parentheses) are as follows: trans, 2.98 ppm (12.6 Hz); cis, 2.93 ppm (11.4 Hz); free, 2.73 ppm (13.0 Hz). The $ZrCl_4$·2$Cl(Me_2N)_2PO$ and free $Cl(Me_2N)_2PO$ concentrations were 0.05 m.

The ^1H NMR temperature dependence of a typical adduct, $ZrCl_4$·2$Cl(Me_2N)_2PO$, will be discussed first (Figure 1). At 231 K, the spectrum of this adduct with an excess of $Cl(Me_2N)_2PO$ in $CHCl_3$ shows three doublets centered at 2.98, 2.93, and 2.73 ppm. At this low temperature there is almost no exchange, and the doublets, due to $^3J(^1H-^{31}P)$ coupling, can be assigned to the trans, cis, and free ligands, respectively. Under these conditions of solvent and temperature the isomerization constant, K_{iso} (=[trans]/[cis]), amounts to 1.08. As the temperature is increased, the trans and cis doublets broaden and eventually coalesce, indicating that a cis–trans isomerization process occurs first. This observation is fundamentally different from that observed for the TiX_4·2L and SnX_4·2L adducts, where the cis–free ligand process is the fastest. A further increase in temperature, above 275 K, results in the broadening of the coalesced cis–trans doublet and the free ligand doublet. The source of this second broadening could be a ligand-exchange reaction between the cis or trans isomer and the free ligand, and in this particular case, NMR spectroscopy cannot identify which exchange is occurring. However, as will be shown later, it can be assigned to the intermolecular ligand exchange between the *trans*-$ZrCl_4$·2$Cl(Me_2N)_2PO$ and $Cl(Me_2N)_2PO$.

The NMR-determined residence times are related to the kinetic equations in the following way.

For the cis–trans isomerization reaction (eq 1) the inverse residence time of L on the cis isomer, $1/\tau_i^r$, is equal to the inverse mean lifetime of the cis isomer for this reaction and equal to the isomerization rate constant, k_i, assuming a first-order rate law:

$$1/\tau_i^r = 1/\tau_i(\textit{cis}\text{-}MCl_4\cdot 2L \rightarrow \textit{trans}\text{-}MCl_4\cdot 2L) = -d[\textit{cis}\text{-}MCl_4\cdot 2L]/dt[\textit{cis}\text{-}MCl_4\cdot 2L] = k_i \quad (4)$$

For the ligand-exchange reactions between the coordinated and free ligand (eqs 2 and 3), first- or second-order, or even mixed, rate laws can be envisaged depending on the reaction mecha-

(14) McIvor, R. A.; McCarthy, G. D.; Grant, G. A. *Can. J. Chem.* **1956**, *34*, 1819.
(15) Lester, P. *Chem. Abstr.* **1955**, *49*, 6300g.
(16) Michaelis, A. *Liebigs Ann. Chem.* **1903**, *326*, 179.
(17) Pisaniello, D. L.; Helm, L.; Meier, P.; Merbach, A. E. *J. Am. Chem. Soc.* **1983**, *105*, 4528.
(18) Frey, U.; Helm, L.; Merbach, A. E. *High-Pressure Res.*, in press.
(19) Ammann, C.; Meier, P.; Merbach, A. E. *J. Magn. Reson.* **1982**, *46*, 319.
(20) Meyer, F. K.; Merbach, A. E. *J. Phys. E* **1979**, *12*, 185.
(21) Abel, E. W.; Coston, T. P. J.; Orrel, K. G.; Sick, S.; Stephenson, D. *J. Magn. Reson.* **1986**, *69*, 92.
(22) Delpuech, J. J.; Ducom, J.; Michon, V. *Bull. Soc. Chim. Fr.* **1971**, 1848.

Table I. Rate Laws and Activation Parameters for Ligand Exchange and Cis–Trans Isomerization of $MCl_4 \cdot 2L$ (M = Zr, Hf) in $CHCl_3$[a]

adduct $MCl_4 \cdot 2L$	K_{iso}[b]	rate const[c]	$\Delta H^{\ddagger}$, kJ mol^{-1}	$\Delta S^{\ddagger}$, J K^{-1} mol^{-1}	$\Delta G^{\ddagger}$(298 K), kJ mol^{-1}	$\Delta V^{\ddagger}$, cm^3 mol^{-1}
$ZrCl_4 \cdot 2Me_2O$[d]	0.00	k_{c2}	28.1 ± 2.3	−100.3 ± 9.2	58.0 ± 0.4 (214–290 K)[e]	
$ZrCl_4 \cdot 2Cl_2(Me_2N)PO$	0.00	k_{c1}	58.9 ± 10.6	−48.8 ± 34.1	73.6 ± 0.9 (267–340 K)	
		k_{c2}	34.5 ± 5.5	−93.0 ± 17.9	62.6 ± 0.4 (267–339 K)	
$ZrCl_4 \cdot 2Cl(MeO)_2PO$	0.03	k_{c2}	27.6 ± 1.3	−113.2 ± 6.0	61.2 ± 0.4 (240–313 K)	
$ZrCl_4 \cdot 2(MeO)_3PO$	2.04	k_i	48.0 ± 1.7	−36.6 ± 6.7	58.9 ± 0.3 (244–276 K)	−1.6 ± 0.6 (260.7 K)
		k_{t2}	30.2 ± 0.8	−96.9 ± 2.8	59.1 ± 0.1 (240–313 K)	−11.1 ± 0.8 (279.1 K)
$ZrCl_4 \cdot 2Cl(Me_2N)_2PO$	1.08	k_i	56.5 ± 4.6	−10.0 ± 18.4	57.7 ± 0.8 (240–260 K)	
		k_{c2}	33.5 ± 1.7[f]	−97.3 ± 5.4[f]	61.7 ± 1.3 (262–355 K)[f]	
$HfCl_4 \cdot 2Cl_2(Me_2N)PO$	0.20	k_{c1}	76.1 ± 0.4	+13.4 ± 1.3	72.8 ± 0.4 (275–339 K)	
		k_{c2}	37.2 ± 2.1	−79.5 ± 0.4	57.3 ± 0.4 (275–339 K)	
$HfCl_4 \cdot 2Cl(MeO)_2PO$	0.40	k_i	67.8 ± 7.9	+14.2 ± 29.7	64.4 ± 1.3 (250–300 K)	
		k_{c2}	20.1 ± 1.7	−131.4 ± 5.4	59.0 ± 0.4 (240–345 K)	
		k_{t2}	26.4 ± 0.9	−99.2 ± 3.3	56.1 ± 0.4 (240–345 K)	
$HfCl_4 \cdot 2(MeO)_3PO$	3.20	k_i	49.6 ± 1.9	−49.6 ± 6.7	64.3 ± 0.1 (270–303 K)	
		k_{t2}	43.1 ± 3.4	−67.4 ± 11.3	63.2 ± 0.1 (283–344 K)	
$HfCl_4 \cdot 2Cl(Me_2N)_2PO$	2.00	k_i	63.2 ± 2.5	−13.0 ± 8.8	66.1 ± 1.3 (265–319 K)	

[a] The errors given are ±1σ. [b] K_{iso} = [*trans*-$MCl_4 \cdot 2L$]/[*cis*-$MCl_4 \cdot 2L$], at ≈220 K; see ref 3. [c] See eqs 4–6 for the corresponding reactions and rate laws. Units: k_{c2}, s^{-1} m^{-1}; k_{c1}, s^{-1}; k_i, s^{-1}; k_{t2}, s^{-1} m^{-1}. [d] In dichloromethane. [e] The temperature range in which the rate constants were determined. [f] In 1,1,2,2-tetrachloroethane: $\Delta H^{\ddagger}$ = 45.6 ± 2.5 kJ mol^{-1}, $\Delta S^{\ddagger}$ = −74.1 ± 7.1 J K^{-1} mol^{-1}, $\Delta G^{\ddagger}$ = 67.8 ± 0.8 kJ mol^{-1}, and the temperature range = 313–393 K.

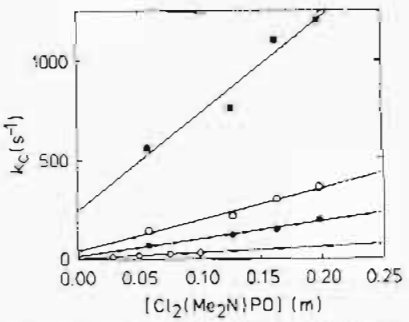

Figure 2. Rate constants, k_c, as a function of free ligand concentration for intermolecular ligand exchange on *cis*-$ZrCl_4 \cdot 2Cl_2(Me_2N)PO$ in $CHCl_3$ at different temperatures: (○) 278.4 K, (●) 305.2 K, (□) 316.2 K, (■) 339.2 K. The $ZrCl_4 \cdot 2Cl_2(Me_2N)PO$ concentration was 0.05 m, except at 278.4 K where it was 0.025 m.

nism(s). The factor of 2 in the NMR-determined inverse residence time of L is due to the fact that only one of the two ligands exchanges at any given time:

$$2/\tau_c^r = 1/\tau_c(cis\text{-}MCl_4 \cdot 2L \rightarrow L) = d[cis\text{-}MCl_4 \cdot 2L]/dt[cis\text{-}MCl_4 \cdot 2L] = k_c = k_{c1} + k_{c2}[L] \quad (5)$$

$$2/\tau_t^r = 1/\tau_t(trans\text{-}MCl_4 \cdot 2L \rightarrow L) = d[trans\text{-}MCl_4 \cdot 2L]/dt[trans\text{-}MCl_4 \cdot 2L] = k_t = k_{t1} + k_{t2}[L] \quad (6)$$

The rate laws for the isomerization and ligand-exchange reactions of the adducts have been determined by measuring the inverse ligand residence times in the different sites as a function of free ligand and/or adduct concentration. The activation enthalpy and entropy, $\Delta H^{\ddagger}$ and $\Delta S^{\ddagger}$, were obtained by measuring the temperature dependence of the various rate constants and fitting the results to the Eyring equation. Linear plots of $\ln(k/T)$ versus $1/T$ were obtained for all the systems studied. The activation volume, $\Delta V^{\ddagger}$, was determined by analysis of the pressure dependence of the rate constants at a given temperature. For the reactions studied at variable pressure the data could be fitted to linear eq 7 (assuming that the activation volume is independent

$$\ln k = \ln k_0 - \Delta V^{\ddagger} P/RT \quad (7)$$

of pressure), where k is the rate constant at pressure P and k_0 is the adjusted rate constant at zero pressure. The rate laws and activation parameters obtained in this study are summarized in Table I.

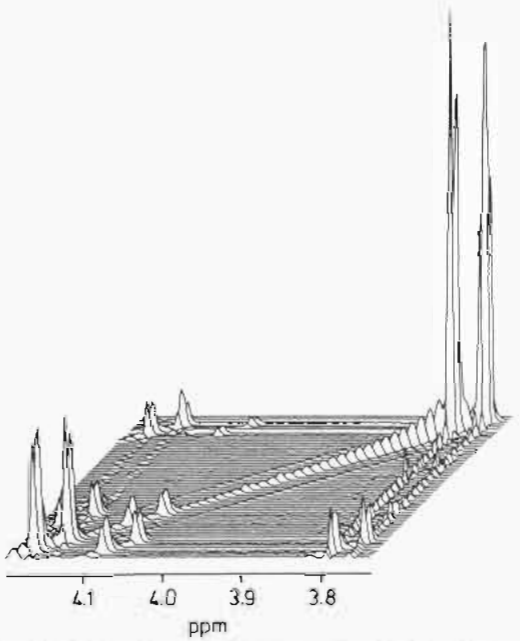

Figure 3. 400-MHz 2-D ^{1}H EXCSY spectrum for the intermolecular exchanges between free $(MeO)_3PO$ and both cis- and trans-coordinated ligand on $ZrCl_4 \cdot 2(MeO)_3PO$ and the intramolecular cis–trans isomerization in chloroform at 248 K. The $ZrCl_4 \cdot 2(MeO)_3PO$ and free $(MeO)_3PO$ concentrations were 0.095 and 0.195 m, respectively.

The adduct *cis*-$ZrCl_4 \cdot 2Me_2O$ shows the simplest kinetic behavior of all the systems studied. The rate law for the free ligand exchange on this single isomer (eq 2) has been determined at three temperature (238.2, 256.7, 264.2 K) while the Me_2O concentration was varied between 0.16 and 0.80 m. The observed k_c values (eq 5) are directly proportional to $[Me_2O]$, indicating a second-order rate law: first order in adduct and first order in ligand.

For *cis*-$ZrCl_4 \cdot 2Cl_2(Me_2N)PO$ there is also only a single two-site exchange (eq 2). However, in this case the plots of k_c versus $[Cl_2(Me_2N)PO]$ do not go through the origin (Figure 2). Thus we have two ligand-exchange pathways, characterized by first- and second-order rate laws. In the $HfCl_4$ solution with the same ligand there is a small amount, <15%, of the trans isomer in $CHCl_3$. However the isomerization reaction could not be followed quantitatively by ^{1}H NMR spectroscopy due to the very rapid coalescence of the small trans doublet with the cis doublet (temperature range ≈ 7 K). The intermolecular exchange of free ligand for *cis*-$HfCl_4 \cdot 2Cl_2(Me_2N)PO$ could be studied between 275 and 339 K and shows the same rate law behavior as that for the $ZrCl_4$

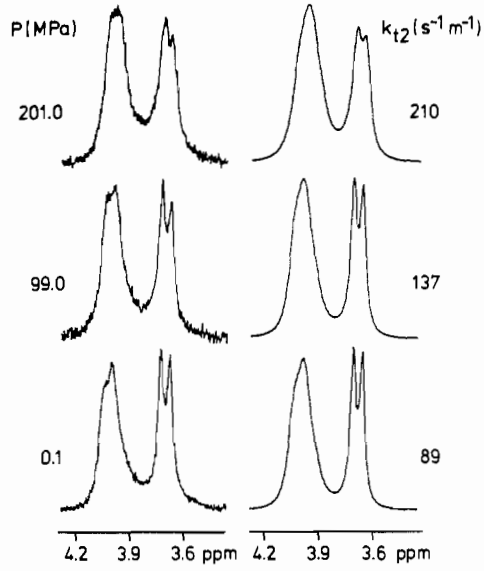

Figure 4. Experimental, left, and calculated, right, 200-MHz ^1H NMR spectra of $ZrCl_4 \cdot 2(MeO)_3PO$ with excess ligand in $CHCl_3$ at 279.1 K as a function of pressure, showing the increase in exchange rate between the trans and free ligand sites as the pressure is increased. The $ZrCl_4 \cdot 2(MeO)_3PO$ and free $(MeO)_3PO$ concentrations were 0.08 and 0.11 m, respectively.

adduct. For all other adducts examined in this study, the intermolecular exchange reactions are second-order processes.

The adduct *cis*-$ZrCl_4 \cdot 2Cl(MeO)_2PO$ is in equilibrium with a very small (<3%) amount of the trans isomer. The coalescence between the two isomers occurs rapidly, in a 5 K temperature interval. The coalescence between the remaining doublets, assigned to the cis-adduct/free ligand exchange reactions, was studied at three temperatures (264.2, 297.0, 323.5 K) as a function of $[Cl(MeO)_2PO]$, from 0.026 to 0.106 m. The exchange rate law is purely second order.

For the *cis*- and *trans*-$ZrCl_4 \cdot 2(MeO)_3PO$ adducts (K_{iso} = 2.04 at 220 K) there is a slight overlap between the low- (eq 1) and high-temperature (eqs 2 and 3) coalescence processes. In this case too (cf. $ZrCl_4 \cdot 2Cl(Me_2N)_2PO$) NMR line broadening can hardly quantify the individual contributions of the three exchange reactions to the observed spectra. The 2-D ^1H NMR exchange spectrum (Figure 3) of a $ZrCl_4 \cdot 2(MeO)_3PO$ solution with excess $(MeO)_3PO$, in chloroform at 248 K, is very useful for this purpose. Under these conditions the three exchange processes occur. Crosspeaks relate: the doublets of the cis and trans isomers (k_{iso} = 3.8 s^{-1}), the doublets of the trans and free ligands (k_{t2} = 9.4 mol^{-1} s^{-1}) and the doublets of the cis and free ligands (k_{c2} = 2.3 mol^{-1} s^{-1}). This last process (eq 2), which represents less than 10% of the total intermolecular exchange processes (eqs 2 and 3), was therefore neglected in the line-broadening simulations of the variable-temperature and variable-pressure data for this adduct. It could also be shown by varying $[(MeO)_3PO]$ between 0.15 and 0.60 m at 251.7 and 291.2 K that the isomerization process obeys a first-order rate law, whereas the intermolecular ligand-exchange process on the trans adduct was second order. The pressure effect on the system was also studied, and some experimental and simulated spectra are illustrated in Figure 4. The resulting pressure-dependence plots are given in Figure 5 and show clearly that both processes are accelerated with pressure but that the effect is much larger for the intermolecular reaction, indicating a bond-making process at the transition state. Both activation volumes are reported in Table I.

For the $HfCl_4 \cdot 2(MeO)_3PO$ and the $ZrCl_4 \cdot 2Cl(Me_2N)_2PO$ adducts, exchange of the free ligand on the cis isomer could be neglected for the same reasons as given for the $ZrCl_4 \cdot 2(MeO)_3PO$ adducts. For the $HfCl_4 \cdot 2Cl(Me_2N)_2PO$ adduct the intermolecular exchange was too slow to be measured in the temperature range studied. The $HfCl_4 \cdot 2Cl(MeO)_2PO$ adduct has a comportment that is unique in this study. In fact, for this adduct, it was not

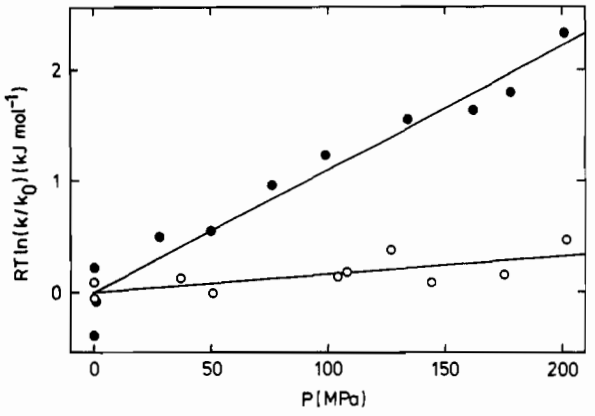

Figure 5. Plot of $RT \ln (k/k_0)$ vs pressure for the ligand-exchange reactions on $ZrCl_4 \cdot 2(MeO)_3PO$ in $CHCl_3$: (○) cis–trans isomerization at 260.7 K, (●) trans–free ligand exchange at 279.1 K. The $ZrCl_4 \cdot 2(MeO)_3PO$ and free $(MeO)_3PO$ concentrations were 0.08 and 0.11 m, respectively.

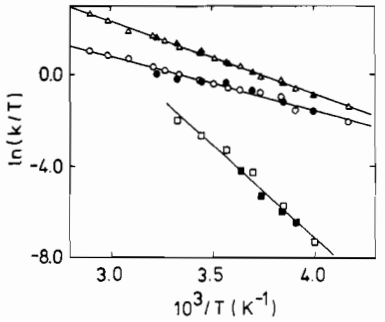

Figure 6. Eyring plots for the ligand-exchange reactions on $HfCl_4 \cdot 2Cl(MeO)_2PO$ in $CHCl_3$ obtained at 60 MHz (open symbols) and 400 MHz (solid symbols): (□) cis–trans isomerization, (○) cis–free ligand exchange, (△) trans–free ligand exchange. The $HfCl_4 \cdot 2Cl(MeO)_2PO$ and free $Cl(MeO)_2PO$ concentrations were 0.05 and 0.06 m, respectively.

possible to simulate the experimental spectra by adjusting only two rate constants. Successful simulations required the simultaneous occurrence of the three possible exchange reactions (eqs 1–3) be taken into account. This behavior was confirmed by doing the study at both 60 and 400 MHz. The Eyring plots are shown in Figure 6.

Discussion

Cis–Trans Isomerization. Frequently ligand rearrangements in octahedral metal complexes have been observed to occur by means of a mechanism involving prior ligand dissociation,[23-30] with reorganization of the five-coordinate intermediate. Variable-pressure kinetics has recently been successfully applied to the study of *ttt*- to *ccc*-$RuCl_2(CO)_2(PR_3)_2$ and of *trans*- to cis-$RuCl_2(CO)(PR_3)_3$ isomerization processes.[31] In both cases the large positive activation volumes of +19 cm^3 mol^{-1} and +16 cm^3 mol^{-1}, respectively, indicate a mechanism that is primarily dissociative in nature. It was concluded that the mechanism involved initial loss of a CO trans to CO in the first reaction and the loss of a

(23) Darensbourg, D. J.; Darensbourg, M. Y.; Dennenberg, R. J. J. *J. Am. Chem. Soc.* **1971**, *93*, 2807.
(24) Darensbourg, D. J.; Nelson, H. H., III. *J. Am. Chem. Soc.* **1974**, *96*, 6511.
(25) Darensbourg, D. J.; Murphy, M. A. *J. Am. Chem. Soc.* **1977**, *99*, 896.
(26) Dobson, G. R.; Asali, K. J.; Marshall, J. L.; McDaniel, C. R. *J. Am. Chem. Soc.* **1977**, *99*, 8100.
(27) Atwood, J. D.; Brown, T. L. *J. Am. Chem. Soc.* **1975**, *97*, 3380.
(28) Cohen, M. A.; Brown, T. L. *Inorg. Chem.* **1976**, *15*, 1417.
(29) Poliakoff, M. *Inorg. Chem.* **1976**, *15*, 2892.
(30) Dobson, G. R.; Asali, K. J. *J. Am. Chem. Soc.* **1979**, *101*, 5433.
(31) Krassowski, D. W.; Nelson, J. H.; Brower, K. R.; Havenstein, D.; Jacobson, R. A. *Inorg. Chem.* **1988**, *27*, 4294.

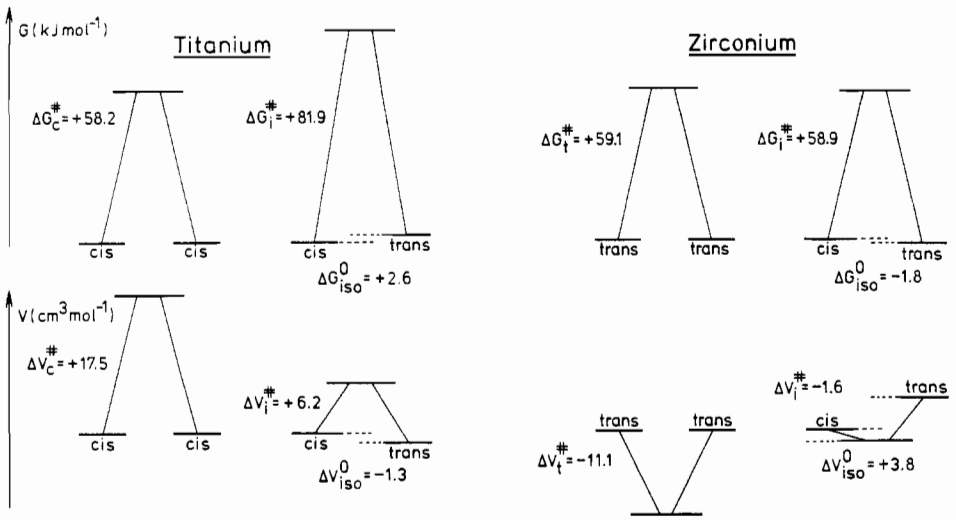

Figure 7. Volume, V, and free energy, G(298 K), reaction profiles for coordinated–free ligand exchange and cis–trans isomerization on $TiCl_4 \cdot 2(MeO)_3PO$ and $ZrCl_4 \cdot 2(MeO)_3PO$ in $CHCl_3$.

phosphine trans to CO in the second reaction.

There is however increasing awareness that ligand permutation in octahedral metal complexes can occur by intramolecular mechanisms involving trigonal-prismatic or bicapped-tetrahedral intermediates.[32-37] These intramolecular mechanisms may be differentiated by means of their activation parameters, by their response to alterations in the electronic and steric character of the coordinated ligands,[33] or even better by 2-D NMR experiments.[37] Two limiting pathways may be envisaged, a first one involving primarily a reorganization without metal–ligand bond breaking and a second one involving a great deal of metal–ligand bond lengthening. This latter process would be expected to prevail when metal–ligand bond dissociation is favored. Proposed examples for these limiting intramolecular cis–trans isomerizations are $W(CO)_4(^{13}CO)PR_3$[34] and $Cr(CO)_4(^{13}CO)PR_3$,[33] respectively. As expected for intramolecular processes, no ^{13}C incorporation from free CO into the $M(CO)_5PR_3$ derivatives was observed during these ligand rearrangements.

For all the $MX_4 \cdot 2L$ (M = Zr, Hf) derivatives showing cis–trans equilibria and kinetically examined in this study, the isomerization process (eq 1) is faster than the intermolecular exchange between free ligand and either the cis or the trans isomer. The isomerization shows rate laws that are first order in adduct with no concentration dependence in free ligand and with $\Delta S^{\ddagger}_{i}$ values between −49 J K^{-1} mol^{-1} and +14 J K^{-1} mol^{-1} (see Table I). We thus suggest an intramolecular rearrangement, possibly via a trigonal-twist process. This is further supported by the very small pressure accelerated *cis*- to *trans*-$ZrCl_4 \cdot 2(MeO)_3PO$ isomerization reaction, leading to a $\Delta V^{\ddagger}_{i}$ of −1.6 ± 0.6 cm^3 mol^{-1} (ΔV°_{iso} = +3.8 ± 0.4 cm^3 mol^{-1} at 244 K). The albeit small, but clearly negative, activation volume indicates that the rearrangement occurs via a slightly contracted six-coordinate transition state. This behavior contrasts with that of the $TiCl_4 \cdot 2L$[7] and $SnCl_4 \cdot 2L$[8-10] adducts for which, first, the intermolecular exchange on the cis isomer is much faster than the isomerization process and, second, the isomerization process itself is characterized by a clearly positivie activation volume (see Figure 7). For the Ti(IV) and Sn(IV) adducts an intramolecular mechanism was also concluded, but this time with an expanded six-coordinate transition state. This is not surprising considering the observation of a D mechanism with a very large $\Delta V^{\ddagger}_{c}$ of +17.5 ± 1.2 cm^3 mol^{-1} for the intermolecular ligand exchange on the *cis*-$TiCl_4 \cdot 2(MeO)_3PO$ adduct.[7]

Intermolecular Ligand Exchange on the $MCl_4 \cdot 2L$ (M = Zr, Hf) Adducts. As discussed above, the cis–trans isomerization process occurring in solutions of *cis*- and *trans*-$MCl_4 \cdot 2L$ adducts in the presence of an excess of ligand, L, is faster than the intermolecular exchange between the free ligand and either the trans and/or the cis adduct. When both intermolecular exchanges occur (eqs 2 and 3), the exchange on the trans isomer is the faster. These intermolecular processes obey second-order rate laws, except in the case of *cis*-$MCl_4 \cdot 2Cl_2(MeN)PO$ (M = Zr, Hf), where a further intermolecular pathway, independent of free ligand concentration, results in a mixed rate law (eq 5).

The second-order intermolecular exchange pathways show very negative $\Delta S^{\ddagger}_{t2}$ and $\Delta S^{\ddagger}_{c2}$ values (between −131 and −67 J K^{-1} mol^{-1}; see Table I) and in the only case studied, *trans*-$ZrCl_4 \cdot 2(MeO)_3PO$, a $\Delta V^{\ddagger}_{t2}$ value of −11.1 cm^3 mol^{-1}. This activation volume contrasts sharply with those ranging from +17.5 to +38.4 cm^3 mol^{-1} found for intermolecular cis–free ligand exchange on $TiCl_4 \cdot 2L$ (L = $(MeO)_3PO$, Me_2O, Me_2Se)[4] and $SnCl_4 \cdot 2Me_2S$,[10] which, together with other evidence, are indicative of a D mechanism. However, it is comparable to those ranging between −10 and −20 cm^3 mol^{-1} found for the intermolecular ligand-exchange reactions of L = Me_2S, Me_2Se, and Me_2Te on $MX_5 \cdot L$ adducts (M = Nb, Ta; X = Cl, Br),[37] which observations were taken as evidence for an I_a mechanism, without ruling out a possible limiting A mechanism. Similarly, we propose an I_a mechanism for the second-order ligand-exchange pathway on *trans*- and *cis*-$MCl_4 \cdot 2L$ adducts.

The first-order cis-exchange pathway is only observed for the less stable phosphoryl adducts in our study, $MCl_4 \cdot 2Cl_2(Me_2N)PO$.[3] It is characterized by clearly more positive $\Delta S^{\ddagger}_{c1}$ values than those observed for the second-order process (see Table I), leading us to suggest a D mechanism. To understand this dual mechanism, it is important to recall the stability sequence of these adducts, $Cl_2(Me_2N)PO < Cl(MeO)_2PO < (MeO)_3PO < Cl(Me_2N)_2PO$, and to note that the difference in the free energies of formation, between the less stable (L = $Cl_2(Me_2N)PO$) and most stable (L = $Cl(Me_2N)_2PO$) $MCl_4 \cdot 2L$ adduct, is more than 40 kJ mol^{-1} at 298 K.[3] For a D mechanism, a linear free energy relationship with slope of ca. −1 should exist between the free energy of activation $\Delta G^{\ddagger}$ and of the free energy of formation ΔG°.[39] If the same is true for Zr and Hf, the increase in the free energy of activation, $\Delta\Delta G^{\ddagger}_{D}$ for the D pathway, from the $Cl_2(Me_2N)PO$ to the $Cl(Me_2N)_2PO$ adducts, should also be in the region of 40 kJ mol^{-1}. Since $\Delta G^{\ddagger}_{I_a}$ is practically constant (see Table I), the

(32) Darensbourg, D. J. *Inorg. Chem.* **1979**, *18*, 14.
(33) Darensbourg, D. J.; Gray, R. L. *Inorg. Chem.* **1984**, *23*, 2993.
(34) Dombek, B. D.; Angelici, R. J. *J. Am. Chem. Soc.* **1976**, *98*, 4110.
(35) Darensbourg, D. J.; Darensbourg, M. Y.; Gray, R. L.; Simmons, D. L.; Arndt, W. *Inorg. Chem.* **1986**, *25*, 880.
(36) Dobson, G. R.; Awad, H. A.; Basson, S. S. *Inorg. Chim. Acta* **1986**, *118*, L5.
(37) Ismail, A. A.; Saurvol, F.; Butler, I. S. *Inorg. Chem.* **1989**, *28*, 1007.
(38) Vanni, H.; Merbach, A. E. *Inorg. Chem.* **1979**, *18*, 2758.
(39) Langford, C. H.; Gray, H. B. In *Ligand Substitution Processes*; W. A. Benjamin Inc.: New York, 1965; p 61.

resulting difference in the free energy of activation between both pathways, $\Delta G^{\ddagger}_{D} - \Delta G^{\ddagger}_{I_a}$, will increase considerably as the stability of the adduct increases. This explains why the dissociative pathway is only observed for the less stable adducts of the phosphoryl ligand series. Such a ligand-triggered, dissociative–associative mechanism cross-over has already been observed[39] for ligand exchange on MX_5·L adduct (M = Nb^{5+}, Ta^{5+}), and a linear free energy relationship with slope of ≈−1 was found between $\Delta G^{\ddagger}$ and ΔG° for their dissociative first-order ligand exchange.

It has been shown by vibrational spectroscopy[3] that the $ZrCl_4$ adducts with the dimethyl chalcogenides Me_2Y (Y = O, S, Se) exist only in the cis form. Intermolecular exchange of Me_2O on *cis*-$ZrCl_4$·$2Me_2O$ obeys a second-order rate law and has a very negative $\Delta S^{\ddagger}_{c2}$ value, indicative of an I_a mechanism. The exchange rates on the *cis*-$ZrCl_4$·$2Me_S$ and *cis*-$ZrCl_4$·$2Me_2Se$ adducts were too fast to be measured, probably due to the increase in nucleophilicity of the sulfide and selenide Lewis bases.

In conclusion, intermolecular ligand exchange on the adducts MCl_{6-n}·nL (M = d^0 transition-metal ion) will obey mechanisms that depend on the nature of the metal M and the exchanging ligand L. Adducts of the second (Nb^{5+}[40] and Zr^{4+}) or third (Ta^{5+}[40] and Hf^{4+}) transition series show a greater tendency toward associative activation modes, whereas adducts of the first transition series (Ti^{4+}[4]) show dissociative activation. Adducts of d^{10} metal ions (Sn^{4+}[7-9] and Sb^{5+}[41]) show the same behavior as Ti^{4+}, i.e. D mechanisms. For the MCl_4·2L adducts the cis–trans isomerization is intramolecular, with an expanded transition state for Ti^{4+} and Sn^{4+} and a contracted transition state for Zr^{4+} and Hf^{4+}. Figure 7 illustrates these observations for coordinated–free ligand exchange and cis–trans isomerization on $TiCl_4$·$2(MeO)_3PO$ and $ZrCl_4$·$2(MeO)_3PO$. It exemplifies the striking differences in reaction mechanism due to the increase in ionic radius, which favors the changeover from a dissociative to an associative activation mode.

Acknowledgment. We thank the Swiss National Science Foundation for financial support through Grant No. 2.672-0.87.

Supplementary Material Available: Tables of inverse ligand residence times as a function of free ligand and/or adduct concentration and tables of temperature and/or pressure dependence of the various rate constants (17 pages). Ordering information is given on any current masthead page.

(40) Good, R.; Merbach, A. E. *Inorg. Chem.* **1975**, *14*, 1030.

(41) Kessler, J. E.; Knight, C. T. G.; Merbach, A. E. *Inorg. Chim. Acta* **1986**, *115*, 85.

Contribution from the Department of Chemistry, University of Florida, Gainesville, Florida 32611

The Role of One-Parameter Plots in a Two-Parameter World

Russell S. Drago

Received August 29, 1989

The simplicity of analysis, ease of presentation, and ready extension to new bases (or acids) have led many investigators to choose a one-parameter analysis to interpret physicochemical measurements. Though it is commonly accepted that two factors contribute to donor or acceptor properties, one-parameter correlations often work because much chemistry is dominated by electrostatic interactions. An improved set of enthalpy-based parameters are presented for such analyses as alternatives to donor numbers, Kamlet–Taft β values, and pK_B data. The conditions that must apply in order for a one-parameter analysis to be valid are described, and criteria are offered to indicate when a one-parameter analysis can be misleading. It is shown that an improper estimate of the covalency in a physicochemical measurement relative to that in the basicity scale utilized can lead to deviations in plotted data which could lead an investigator to improperly conclude that steric effects or metal to ligand π-back-bonding exists.

Introduction

In 1965, we published[1] an analysis of the solution enthalpies for reactions of donors with acceptors to form 1:1 adducts in nonpolar, nonbasic solvents, where solvation contributions are minimal. A one-term equation cannot possibly accommodate even the limited data set which indicates a donor order toward iodine of $R_3N > R_2S > R_2O$ and one toward phenol of $R_3N > R_2O > R_2S$. A two-term E and C (electrostatic and covalent) equation was found[1,2] to be sufficient for the correlation of these as well as over 500 other enthalpies of adduct formation.

$$-\Delta H = E_A E_B + C_A C_B - W \qquad (1)$$

Empirical E_A, E_B, C_A, C_B, and W parameters are reported[3] for the acids and bases to correlate these enthalpies. W represents a constant contribution to the enthalpy; W for an acid is independent of the base employed. The essential conclusion of this treatment is that there is no single reference acid (or base) that can lead to reference parameters that provide an inherent order of basicity (or acidity). For example, it was shown[4] that the Kamlet–Taft β parameters[5] are a special case of the E and C equation that applies to mainly electrostatic acids or acid properties. They fail to correlate systems with more appreciable covalent contributions.

The various donor orders that can result for a series of bases as the type of acid varies can be illustrated by factoring and rearranging eq 1 as described by Cramer and Bopp:[6]

$$\frac{-\Delta H + W}{C_A + E_A} = \frac{C_B + E_B}{2} + \left(\frac{C_B - E_B}{2}\right)\left(\frac{C_A - E_A}{E_A + C_A}\right) \qquad (2)$$

With use of the reported E and C parameters, the graph in Figure 1 can be constructed as described in ref 7. Different acids are

(1) Drago, R. S.; Wayland, B. B. *J. Am. Chem. Soc.* **1965**, *87*, 375.
(2) (a) Drago, R. S. *Struct. Bonding* **1973**, *15*, 73. (b) Drago, R. S. *Coord. Chem. Rev.* **1980**, *33*, 251.
(3) Drago, R. S.; Wong, N.; Bilgrien, C.; Vogel, G. C. *Inorg. Chem.* **1987**, *26*, 9.
(4) Doan, P. E.; Drago, R. S. *J. Am. Chem. Soc.* **1982**, *104*, 4524.
(5) Kamlet, M. J.; Abboud, J.-L. M.; Taft, R. W. *Prog. Phys. Org. Chem.* **1981**, *13*, 485. Kamlet, M. J.; Abboud, J.-L. M.; Abraham, M. H.; Taft, R. W. *J. Org. Chem.* **1983**, *48*, 2877 and references therein.
(6) Cramer, R. E.; Bopp, T. T. *J. Chem. Educ.* **1977**, *54*, 612.
(7) The $-\Delta H$ value for a selected base reacting with phenol is calculated from eq 1 by using reported E and C parameters. $-\Delta H$ divided by $C_A + E_A$ is plotted on a graph of $-\Delta H/(C_A + E_A)$ vs $(C_A - E_A)/(C_A + E_A)$. The enthalpy is then calculated with reported parameters for the same base reacting with I_2, the point plotted, and a straight line drawn connecting the points. Equation 2 is that of a straight line, and the calculated enthalpies for all acids interacting with this base will fall on this line. The procedure is repeated for a series of bases diethyl sulfide (51), diethyl ether (40), pyridine (16), *N*-methylimidazole (15), and dimethyl sulfoxide (56), and the resulting plot is shown in Figure 1. (The numerical values in parentheses correspond to the base-numbering scheme in Table I.)

0020-1669/90/1329-1379$02.50/0